Journal of Environmental Chemical Engineering 8 (2020) 103688

Contents lists available at ScienceDirect

Journal of Environmental Chemical Engineering

journal homepage: www.elsevier.com/locate/jece

Indium electrowinning study from sulfate aqueous solution using different metal cathodes

E. Ciro[a,*], A. Dell'Era[b], M. Pasquali[b], C. Lupi[a]

[a] ICMA Department, University Sapienza Rome, Via Eudossiana 18, 00184, Roma, Italy
[b] SBAI, University Sapienza Rome, Via Castro Laurenziano 7, 00161, Roma, Italy

ARTICLE INFO

Keywords:
WEEE
Sulfate electrolyte
Electrowinning
Indium recovery
Recycling

ABSTRACT

Electrowinning represents a promising methodology for recovery of strategical, scarce metals. In this study, an indium electrowinning process using a sulfate electrolyte on stainless steel, nickel, titanium, aluminum and copper (SS, Ni, Ti, Al and Cu) cathodes was investigated. Firstly, cyclic voltammetry carried out at 15 mV/s scanning rate and 25 °C temperature evaluated the suitability of electrolyte and the surface reactivity on different metal cathodes. Subsequently, indium was deposited using a current density of 25 A/m^2 for 22 h at 40 °C and pH 2.3. After electrowinning process, analysis of specific energy consumption (SEC), current efficiency (CE) morphological (SEM/EDX), and crystallographic (XRD) tests on obtained deposits were performed. Cyclic voltammetry results revealed that the chemical reagents of solution stabilize the indium reduction reaction, while Ni cathode showed the highest current intensity for reduction reaction followed by SS, Ti, Cu, and Al. With a significant CE and SEC performance, Ni and SS cathodes reached around 93 % CE and 1.67 kW h/kg SEC, respectively. Referring to Ti cathode, other optimization tests should be performed to enhance obtained results. After deposition process, different surface morphologies and different crystallinity degree can be observed for each deposit, being common the presence of surface defects. The findings of this investigation allowed to determine the most suitable cathode for indium electrowinning from sulfate electrolyte.

1. Introduction

The increasing demand for indium as indium-tin-oxide (ITO) has led this metal to become a strategic material for the international commercial trade of green energy and audiovisual technologies. Many of these applications comprise flat display screens, optical sensor and optoelectronic systems, semiconductors and photovoltaic solar cells [1,2]. Thus, an indium excessive demand and consumption for high-tech applications have made this metal to reach the top of critical materials classification.

In order to facilitate worldwide indium supply, the industrial extraction has commonly been realized from mineral aggregate or by-products in sulfide ores of zinc, copper, tin and lead [3,4]. Belgium, France, Canada, Japan, South Korea and China constitute the most relevant countries in charge of the global production of this metal [5]. Although, these six countries are strongly considered the indium market leaders with an estimated control around 98 % of the primary production in 2015, the South Korea and China are the main indium manufacturer with an annual estimation of 545.000 t [6,7]. The limiting availability combined with excessive demand of this metal proposes an eventual shortage for emerging economies development [7,8]. Primary extraction processes eventually represent severe environmental threats due to polluting drinking water, cultivable grounds, fauna and flora [9]. Therefore, one of the essential current challenges to permit the growth of those emerging market lies in finding alternative raw materials for indium supply.

Waste of electrical and electronic equipment (WEEE) has recently been considered an attractive secondary source to be treated [3,10–12]. Some crucial advantages brought out from WEEE, rather than primary ores, constitute: (i) economic dependence reduction of leading suppliers, (ii) lower energy, chemicals and water consumption, (iii) treatment and benefit of large amounts of metals concentrated into WEEE, and (iv) enhancing occupational health in mining because of hazardous metals absence (Th and U). Also, several researchers have agreed on ITO, with 90 % In_2O_3 and 10 % SnO_2, represents one of the most meaningful indium inputs in WEEE (discarded liquid crystal displays (LCD) of laptops, televisions, touchscreens, and photovoltaic cells, etc.). The content of this metal in LCD modules varies from 100 to 400 ppm [13], then recycling these wastes could contribute for mitigating unbalance supply problems and reaching high incomes for the next years

* Corresponding author.
E-mail address: erwin.ciro@uniroma1.it (E. Ciro).

https://doi.org/10.1016/j.jece.2020.103688
Received 12 September 2019; Received in revised form 21 December 2019; Accepted 12 January 2020
Available online 15 January 2020

[4,14,15]. On the whole, WEEE shows an evident potentiality to become a suitable raw material requiring the development of extractive methodologies capable of guaranteeing an efficient, continuous and affordable recovery process.

Nowadays, many studies have proposed the hydrometallurgy as the best methodology to recover indium from WEEE. Hydrometallurgical processes have often focused on ITO leaching from LCD scraps using acid solutions such as HNO_3, HCl and H_2SO_4, as well as employing indium separation methods as solvent extraction, coagulation, cementation and precipitation [3,16–21]. Another methodology employed to obtain pure indium metal as final process step is electrowinning. This methodology should highlight, at industrial scale, low energy consumptions, reduced environmental effects and high recovery efficiencies. These requirements also involve other challenges in processing associated with electrolytes, electrodes pair selection and cell design. Therefore, the influence of operational parameters such as deposit quality, current density, cathodic material and electrolyte on current efficiency (CE) and specific energy consumption (SEC) needs to be concerned in electrochemical treatments even at lab-scale.

Indium recovery attempts via electrowinning have employed nitric and very extensively chloride electrolytes combined with stabilizing compounds. Galvanostatic recovery, using HNO_3 wastewater baths with an aluminum/cast-iron electrode, a 64 A/m^2 current density, pH lower than 6.1 and 25 °C temperature, to obtain around 90 % of CE and low SEC of about 0.5 kW h/kg, has been performed [21]. Furthermore, electrolytes of $InCl_3-HCl–NaOH–H_2O$ at room temperature with NaCl supporting salt reached about 90 % of CE [22]. Although using these two acid electrolytes in electrowinning is possible to obtain uniform deposits and low SEC, environmental issues endanger the technical and economic process stability. The dangers of chlorine gas require a sealed and expensive system, to avoid dangers for human health. In this regards, significant investments on constant maintenance and specialized electrochemical cell are required to control the poisoning vapor evolution [23] and maintain occupational health and safety of workers. Therefore, different electrolytes with no pollutant and toxic gases emissions and less powerful corrosion effects are proposed as a suitable measure to perform more affordable indium electrowinning. In this case, the use of sulfates does not generate environmental pollution problems as chlorides present, as well as the optimization of electrowinning process could represent an indubitable improvement of the indium recovery.

Another important parameter to be taking into account to perform the indium electrowinning represents the electrolyte composition. Indeed, the assistance of supporting additives such as sodium and aluminum sulfate, and boric acid contribute to regulating both deposit quality and CE [24,25]. Currently, suitable attempts to determine the operative conditions for indium recovery from sulfate electrolyte is slightly considered. Therefore, studies to evaluate proper metal cathodes for indium electrowinning based on deposit morphologies, current efficiency and energy consumption could involve a significant contribution. In the present investigation, all analyses have been performed using a fixed sulfate solution for evaluating the reactivity surface, CE, SEC and deposit surface morphology on different metal cathodes (SS, Ni, Ti, Al and Cu) during indium electrowinning.

2. Materials and methods

2.1. Materials

In this research, the utilized electrolyte was 62 g/L In^{3+} (140 g/L $In_2(SO_4)_3$), 5 g/L H_3BO_3, 30 g/L Na_2SO_4 and 20 g/L $Al_2(SO_4)_3$. All employed reagents presented high purity and were purchased from Carlo Erba Reagents. The bath preparation was permanently supported by stirring up to reach a complete homogenization. Furthermore, subsequent voltammetric and electrowinning tests were performed by using different cathodes: stainless steel (SS, AISI 316 L), nickel (Ni, 99.9 %), titanium (Ti, Grade 2), aluminum (Al) and copper (Cu, 99.9 %).

Table 1
Experimental conditions for cyclic voltammetry tests.

Parameters	Conditions
Chemical composition of electrolyte	62 g/L In^{3+} (140 g/L $In_2(SO_4)_3$), 5 g/L H_3BO_3, 20 g/L $Al_2(SO_4)_3$ and 30 g/L Na_2SO_4.
Cathodes	SS, Ni, Ti, Al and Cu
Reference and counter electrode	SCE (E_{SHE} = +241 mV) and Pt
Output potential	−1.8 to 1.0 V (SCE)
Scan rate	15 mV/s
Temperature	25 °C
pH	2.2

2.2. Cyclic voltammetry study

Cyclic voltammetry tests were carried out by using the sulfate solution at 15 mV/s scanning rate to evaluate the metal cathode reactivity response. In Table 1, it can be seen the experimental conditions used to perform cyclic voltammetry tests. These tests also were supported by a counter electrode of 99.99 % pure platinum. A saturated KCl Calomel Electrode (SCE, E_{SHE} = +241 mV) was employed as a reference electrode at room temperature. The cathodic surfaces with an approximate area of 4 cm^2 were polished by using fine-grained abrasive paper, whereas the counter electrode was washed into a concentrated nitric solution to eliminate pollutants. The cyclic voltammetry study was performed inside a 100 m L-three-electrodes cell connected to a Potentiostat/Galvanostat Amel 2049. The voltage scanning range was established between -1.8 and 1.0 V vs. SCE.

2.3. Indium electrowinning

In order to recover indium from the sulfate electrolyte, an electrowinning process was proposed. In this electrowinning process, SS, Ni, Ti, Cu and Al were used as metal cathodes to carry out indium deposition, while a lead alloy anode (Pb-0.7Ag) closed the system. The electrodes were then fixed at 30 mm distance for all electrowinning experiments. The reduction process was assisted with a current density (25 A/m^2) for 22 h at 40 °C to achieve a high CE, low SEC, and deposit without undesirable dendritic growth. The pH value was also adjusted around 2.3 in order to lessen the hydrogen evolution reaction (HER). Further, the electrowinning process was assisted with constant stirring of the electrolyte at 280 rpm to remove the possible hydrogen bubbles formation on the cathodes.

After the deposits were obtained on SS, Ni, Al, Ti and Cu cathodes, they were subjected to abundant double-distilled water washes to eliminate the presence of the remaining sulfate salts end then dried. Subsequently, the deposit was weighted and analyzed by using Scanning Electron Microscope combined with energy dispersive X-ray analyzer (Hitachi S-2500, SEM/EDS). Furthermore, X-ray diffraction analysis (XRD) assisted with a Cu Kα source: λ = 1.5418 Å was carried out to evaluate the indium deposits crystallinity in the angle range between 30° and 80° with a slow 2θ step size. Finally, the crystallographic phases identification was carried out using the database of Crystallography Open Database (C.O.D).

3. Results and discussion

3.1. Cyclic voltammetry

Fig. 1A-E show cyclic voltammograms of different cathodic surfaces (SS, Ni, Ti, Cu and Al) in a potential range between -1.8 V and 1.0 V vs. SCE. All electrodes show three common reactions during the cyclic voltammetry test: *i*) indium reduction (In^{3+}/In^0), *ii*) HER (H^+/H_2), and *iii*) indium oxidation (In^0/In^{3+}).

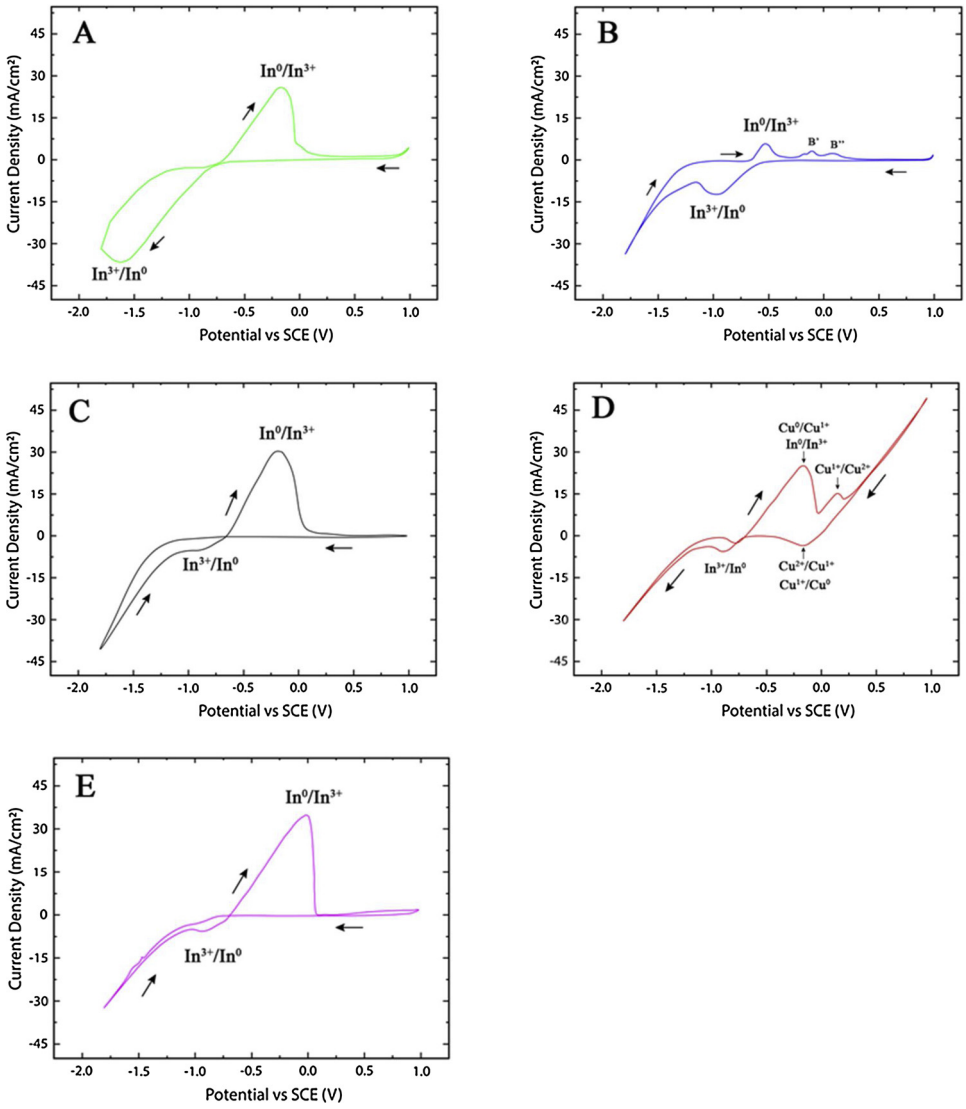

Fig. 1. Evaluation of redox behavior in a sulfate electrolyte at pH 2.2 and 25 °C at 15 mV/s for A) SS, B) Ni, C) Ti, D) Cu and E) Al.

In all voltammograms a cathodic peak formation is present. Ti, Cu and Al show similar behavior of the reduction process without hydrogen evolution with resulting low peak intensity.

Furthermore, all these three metal surfaces present the starting point of plating at -0.65 V. Otherwise, SS and Ni cathodes present greater cathodic reduction peak. Although this could indicate a well-developed concentration gradient near the cathode surface (diffusive conditions), the overlapping of two reduction processes occurs. Thus, a high peak of current intensity is obtained. Ni cathode does not present a well-defined equilibrium potential since the initial cathodic current flowing is due to the HER then at more negative potentials In^{3+} reduction starts. While SS cathode presents a simultaneous HER and In reduction. This behavior also can be seen on charge values in Table 2, where the effective charge on cathodic metal support is represented by higher values due to In^{3+} and H^{+} contemporary reduction reaction.

The Cu cathode shows two crossovers, one is the same starting point previously mentioned, whereas the second one indicates Cu nucleation that was identified at -0.73 V.

Besides, on copper voltammogram, starting from 1 V an increase of the current intensity appears as potential decreases showing the two copper reduction peaks: Cu^{2+}/Cu^{1+} and Cu^{1+}/Cu°. These peaks are identified at -0.01 V and -0.305 V vs. SCE [26], but in this case they overlap. Based on the previous analysis, the highest current intensity for indium reduction is obtained on SS cathode followed by Ni, Al, Cu and Ti cathode, indicating that a greater reactivity is then suggested for SS and Ni.

Table 2
Electrochemical parameters values for different metal support obtained at 15 mV/s in a sulfate electrolyte and 25 °C.

	Metal electrode				
	SS	Ni	Ti	Cu	Al
OCP	0.39	1.32	1.27	0.86	1.31
E_{pc} (V)	−1.62	−0.98	−0.91	−0.88	−0.92
E_{pa} (V)	−0.16	−0.52	−0.18	−0.16	0.01
J_c (mA/cm^2)	−36.59	−12.13	−5.04	−5.89	−1.11
J_a (mA/cm^2)	25.65	5.59	30.85	24.93	35.11
Q_c (μC)	−95.6	−103.2	−115.4	−81.4	−110.2
Q_a (μC)	36.2	8.9	56.5	29.4	56.1

Moreover, other behaviors can be observed in cyclic voltammograms from sulfate solution. The SS, Ti and Al cathodes present similar oxidative behavior with a well-defined indium stripping peak around -0.1 V vs. SCE. Although, all metal supports develop a sharp oxidative peak as the positive potential sweep increases, Ni and Cu supports show additional redox processes. In the case of Ni, after the indium stripping

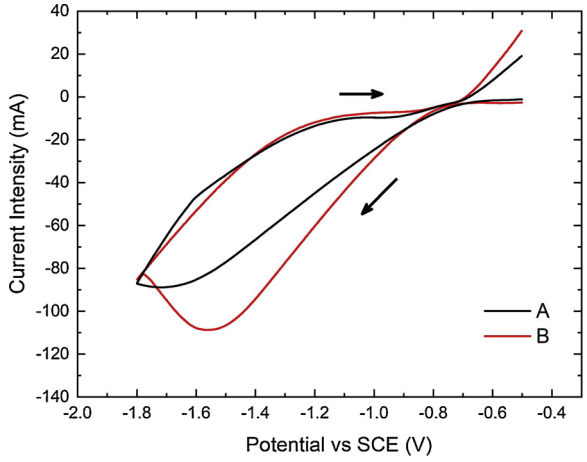

Fig. 2. Effect of indium reduction on SS cathode at 15 mV/s, pH 2.2 and 25 °C using a solution of: A) $In_2(SO_4)_3$; B) $In_2(SO_4)_3$, H_3BO_3, Na_2SO_4 and $Al_2(SO_4)_3$ (the optimized indium solution).

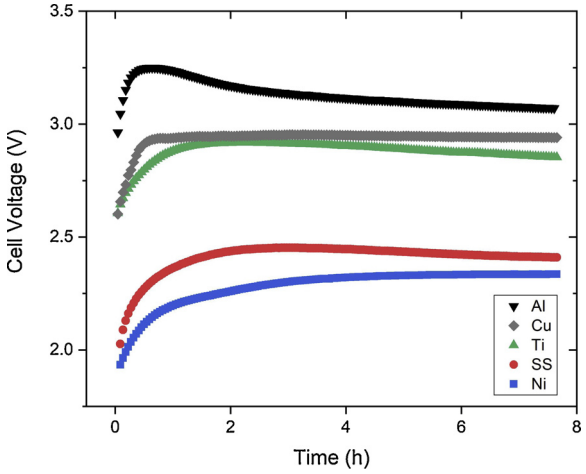

Fig. 3. Cell voltage curves during 8 h of indium electrowinning from the sulfate electrolyte with current density of 25 A/m^2 at 40 °C and pH 2.3 using different cathodic supports.

peak, two other anodic peaks are formed at more positive potentials, which could be related to desorption of indium adatoms from In-Ni physical mixture previously deposited [27,28].

Two oxidation peaks are also present in voltammetry performed on copper. The one at lower anodic potential (-0.18 V) is related to an overlapping of two peaks, due to copper and indium stripping, while the peak at higher potential (0.15 V) is related to Cu^{1+} oxidation [26].

The main electrochemical parameters, for each metal support, obtained by performing voltammetries at 15 mV/s and 25 °C were reported in Table 2.

All the above-mentioned explanation for Fig. 2, it is numerically described in Table 2. In addition, the cathodic and anodic charge on each metal support from the voltammetries at 15 mV/s and 25 °C were also calculated. It is observed that cathodic charge presents values much higher than the anodic ones, which respectively is due to In^{3+} and H^+ contemporary reduction reaction for SS and Ni, while Al, Ti, and Cu present cathodic charge is less important due to the only indium reaction. Thus current efficiency was not calculated and reported on the Table 2 given that an unreliable result referred to a galvanostatic test. By considering galvanostatic test on Ni, it is possible to perform electrowinning at more negative potentials than cathodic peak without reaching the hydrogen evolution by imposing an appropriated current density. By comparing data of current efficiency obtained in galvanostatic test with those obtained by voltammetric test, there is not a suitable agreement. The former gives absolutely the best results, while the latter seems to give the worst one. Thus, current efficiency has not been calculated by charge obtained from voltammetric tests.

On the indium electrowinning other parameters are significant: pH, temperature, electrolyte composition, solution conductibility, complexes formation, current density, and so on. The effect of these parameters also requires to be investigated. For instance, boric acid, conventionally, is added in solution baths acting as a local proton source for shifting the rise of surface pH to higher cathodic potentials improving the electrodeposition [1], furthermore, it is possible to have the presence of complexes among indium and sulfate or other ions [2] that can influence the activity of the indium in solution and then the current efficiency and specific energy consumption. Therefore, the study of effect of the electrolyte composition should be evaluated more in detail. However, in this work, just as an example, the electrolyte composition effect has been simply highlighted. Here we only considered the addition effect of inorganic compounds as boric acid, sodium and aluminum sulfate. While SS cathode has been selected since this metal is affordable, very common and has a good electrochemical performance (as it will be shown in Fig. 3).

In Fig. 2 is shown a voltammetry test was carried out at pH 2.2 and 25 °C. The presence of those compounds such as boric acid, sodium and aluminum sulfate can be clearly highlighted by an increase of current intensity and a decrease of peak potential [24,29]. Additionally, electrowinning tests were also performed and presented in Table 3. From these results, the solution merely prepared with indium sulfate presented an overvoltage cell around 3.0 V, constituting 0.7 V higher than the same test for the optimized solution with stabilizing compounds. There is an evident change on the energy consumption indicating a steep growth of CE close to 93 %, whereas SEC falls up to 1.67 kW h/kg. Thereby, a positive effect of energy consumption can be obtained by using the optimized electrolyte from sulfate solution.

Table 3
Effect of the optimized solution on CE and SEC for A) indium and B) optimized solution.

Test	Current density (A/m^2)	Cell voltage (V)	% CE	SEC (kWh/kg)
A	25	3.00	26.42	7.96
B		2.30	92.46	1.67

3.2. Indium electrowinning

The In electrowinning was carried out by galvanostatic process on different metal cathodes (SS, Ni, Ti, Al and Cu) in order to evaluate CE, SEC, morphology and crystallographic phases of the obtained deposits. In Table 4, it is possible to observe the energy consumption results of the indium deposition using 25 A/m^2 for 22 h at 40 °C and pH 2.3. The results indicate that voltage cell is stabilized around 2.27 V for Ni and SS cathode, whereas Ti, Cu and Al cathodes reach their voltage cell stabilization at higher values as it can be seen in Table 4. In addition, the previous results also are in agreement with those of the overpotential values, indicating lower overpotential values for Ni, followed with a slight difference by SS support. Whereas the other metals

Table 4
The current efficiency and specific energy consumption for the indium electrowinning using 25 A/m^2 as current density for 22 h at 40 °C and pH 2.3.

Cathode	Cell voltage (V)	η (V)	% CE	SEC (kWh/kg)
Ni	2.27 ± 0.01	0.128	95.43	1.67
SS	2.28 ± 0.02	0.131	93.86	1.70
Ti	2.87 ± 0.05	0.314	85.46	2.36
Cu	2.92 ± 0.01	0.329	26.40	7.76
Al	3.12 ± 0.01	0.391	13.92	13.57

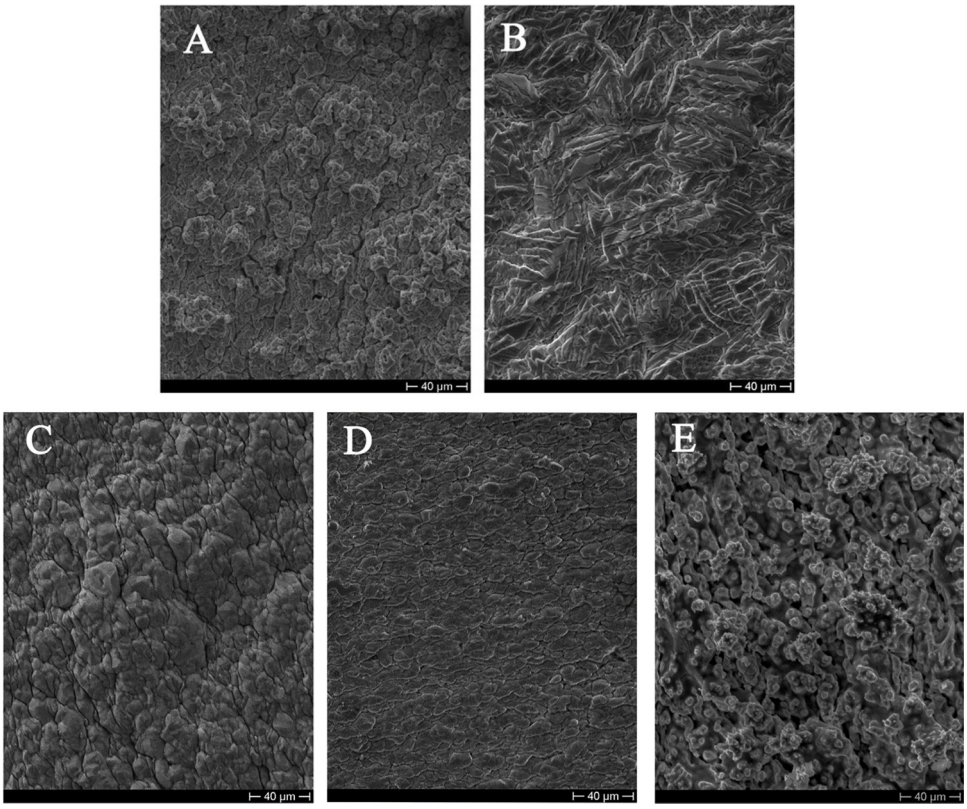

Fig. 4. SEM micrographs of indium deposits obtained by electrowinning process on: A) SS, B) Ti, C) Ni, D) Cu and E) Al by using the aforementioned electrolyte solution (140 g/L $In_2(SO_4)_3$), 5 g/L H_3BO_3, 20 g/L $Al_2(SO_4)_3$ and 30 g/L Na_2SO_4) at 40 °C and 25 A/m^2.

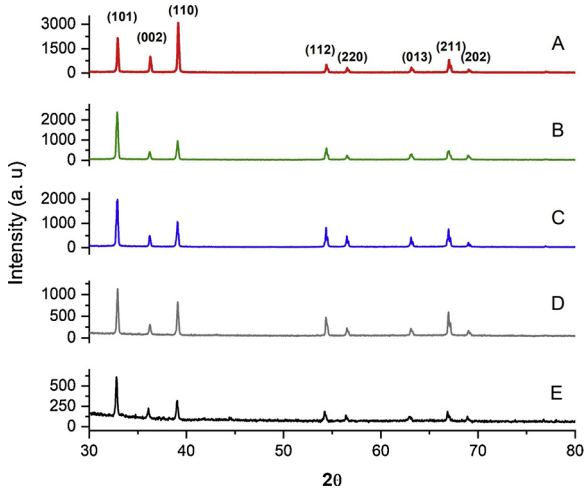

Fig. 5. XRD patterns for the indium deposit obtained on: A) SS, B) Ti, C) Ni, D) Cu and E) Al by using the aforementioned electrolyte solution (140 g/L $In_2(SO_4)_3$, 5 g/L H_3BO_3, 20 g/L $Al_2(SO_4)_3$ and 30 g/L Na_2SO_4,) at 40 °C and 25 A/m^2.

reached values much higher.

Regarding CE, a high percentage of around 94 and 95.5 % are reached by Ni and SS cathode respectively. Subsequently, Ti, Cu and Al (85.46 %, 26.40 % and 13.92 %) showed lower efficiencies. After each deposition process, the final pH value was around 1.5 as a result of the contribution of the H^+ ions from the water oxidation. From literature, other authors have presented current efficiencies lower than those shown in our research, however different experimental parameters and scopes impede a suitable comparative analysis for indium electrowinning from sulfate solutions [24,25,27,30]. Since energy consumption is industrially considered a relevant parameter in electrowinning, Ni and SS cathodes exhibited remarkable results indicating lower SEC around 1.70 kW h/kg (Table 4). Therefore, these two cathodes represent suitable supports to perform the indium electrowinning using an optimized sulfate electrolyte. Additionally, intermediate values for the electrowinning process on Ti propose further investigations to reach the energy consumption optimization; whereas an elevated cathodic overpotential on Al and Cu electrodes shows the worse CE and SEC responses resulting even in scarce deposits.

The cell voltage of the electrowinning process performed at 25 A/m^2 on every electrode with a sulfate electrolyte at 40 °C and pH 2.3 is presented in Fig. 3. These curves display different cell voltages, which after an initial transient voltage reaches the equilibrium stage. The comparison among the different cell voltage highlights the different cathodic overpotential for each metal, being all the other condition maintained equal in all performed tests.

It could say that, at a fixed current density, for having low SEC values it needs, merely, to choose a cathodic support presenting a lower overvoltage. However, another crucial factor influencing SEC values is the related CE. For instance, due to the great HER, Cu has a CE higher and SEC lower than Ti.

3.3. Characterization

In order to have high re-melting efficiency, the deposit aspect and its quality in term of porosity roughness and relative density represent important factors influencing the hydrometallurgical processes. Those parameters together with SEC and CE have the same importance for indium productivity.

Fig. 4 shows the SEM micrographs of the deposit morphologies obtained on SS, Ni, Ti, Al and Cu electrode substrates. Fig. 4A and D depict a plate morphology, which is finer for Cu cathode. The plate microstructure is broadly uniform, and also it can be seen that surface

defects such as cracks and holes generated by hydrogen bubbles detachment are not present.

Likewise, the obtained deposit on Ni cathode shows a lamellar morphology (Fig. 4B). This lamellar morphology was more compacted, unlike the other deposits.

In the same experimental conditions, deposits on Ti showed an irregular grain morphology (Fig. 4C). Finally, in the indium deposition using Al electrode, the micrographs indicate irregular deposits with a thinner dendritic structure combined with the formation of opened cavities with a high porosity. The last deposit, being very thin, reproduces the cathodic substrate morphology, showing the high roughness of Al cathode. Therefore, the deposit obtained on aluminum substrate presents the worse aspect quality.

Fig. 5 shows the XRD pattern for the indium deposit obtained on different cathodic substrates by electrowinning. On the ground of the crystallography outcomes, all deposits present a tetragonal crystalline structure (C.O.D. 1539229). The deposit collected on SS (Fig. 5A) offers higher peak intensities, while the lower ones have been obtained by using aluminum as a substrate (Fig. 5E). In the case of SS cathode, the crystallographic plane for the preferential peak was (110), which corresponds to $2\theta = 39.10^{\circ}$. Whereas in the other cases, the main plane is represented by (101) at $2\theta = 32.96^{\circ}$. Furthermore, it can be observed in the case of Ni and Cu cathode (Fig. 5C and D) the crystallites show a different preferential orientation for secondary peaks respect to those of titanium and aluminum (Fig. 5B and E). The secondary peaks highlight at $2\theta = 54.42^{\circ}$ and 67.11°, and concur with (112) and (211) crystallographic plane, respectively. Besides, other peaks with lower intensity can be seen at $2\theta = 36.33^{\circ}$, 56.64°, 63.14° and 69.20° for crystallographic planes (002), (220), (013) and (202), respectively.

4. Conclusion

Based on the results obtained, a real influence of the material cathode on indium electrowinning processes has been observed:

From voltammetric test, SS and Ni cathodes present higher reactive surface.

From long duration galvanostatic tests SS and Ni show the highest CE values with lowest SEC.

Different morphologies of indium deposit suggest an influence of the type of cathode at the same experimental conditions. The Ni deposit presents the most compact morphology, while aluminum the most porous one.

The most crystalline deposit has been obtained on SS followed by Ni and Ti, while on Al it has the lowest crystallinity.

Finally, it is possible to state that Ni and SS are the most suitable cathodic supports for indium electrowinning from sulfate solution, nevertheless Ti cathode also present significative results and could be employed for further optimization investigations.

CRediT authorship contribution statement

E. Ciro: Conceptualization, Methodology, Writing - review & editing. **A. Dell'Era:** Methodology, Writing - review & editing, Resources, Supervision. **M. Pasquali:** Resources, Supervision. **C. Lupi:** Conceptualization, Writing - review & editing, Resources, Supervision.

Declaration of Competing Interest

The authors declare that they have no known competing financial interests or personal relationships that could have appeared to influence the work reported in this paper.

References

[1] K.J. Schulz, J.H. DeYoung, J.R.R. Seal II, D.C. Bradley, Germanium and indium, Crit. Miner. Resour. United States — Econ. Environ. Geol. Prospect. Futur. Supply, Reston, (2017), pp. I2–I27 Chapter I Virginia.
[2] D. Fontana, F. Forte, R. De Carolis, M. Grosso, Materials recovery from waste liquid crystal displays : a focus on indium, Waste Manag. 45 (2015) 325–333, https://doi.org/10.1016/j.wasman.2015.07.043.
[3] C. Lupi, D. Pilone, In(III) hydrometallurgical recovery from secondary materials by solvent extraction, J. Environ. Chem. Eng. 2 (2014) 100–104, https://doi.org/10.1016/j.jece.2013.12.004.
[4] L. Ciacci, T.T. Werner, I. Vassura, F. Passarini, Backlighting the European indium recycling potentials, J. Ind. Ecol. 23 (2019) 426–437, https://doi.org/10.1111/jiec.12744.
[5] K. Zhang, Y. Wu, W. Wang, B. Li, Y. Zhang, T. Zuo, Recycling indium from waste LCDs : a review, Resources, Conserv. Recycl. 104 (2015) 276–290, https://doi.org/10.1016/j.resconrec.2015.07.015.
[6] C.S. Anderson, Indium Statistics and Information, Indium - MCS 2019 Data Sheet, (2019) 78–79. https://www.usgs.gov/media/files/indium-mcs-2019-data-sheet (accessed September 6, 2019).
[7] A.C. Tolcin, Minerals Yearbook, Indium, Reston, Virginia, 2015https://www.usgs.gov/centers/nmic/indium-statistics-and-information.
[8] A.V.M. Silveira, M.S. Fuchs, D.K. Pinheiro, E.H. Tanabe, D.A. Bertuol, Recovery of indium from LCD screens of discarded cell phones, Waste Manag. 45 (2015) 334–342, https://doi.org/10.1016/j.wasman.2015.04.007.
[9] B. Swain, C.G. Lee, Commercial indium recovery processes development from various e-(industry) waste through the insightful integration of valorization processes: a perspective, Waste Manag. 87 (2019) 597–611, https://doi.org/10.1016/j.wasman.2019.02.042.
[10] A. Dell'Era, M. Pasquali, C. Lupi, F. Zaza, Purification of nickel or cobalt ion containing effluents by electrolysis on reticulated vitreous carbon cathode, Hydrometallurgy 150 (2014) 1–8, https://doi.org/10.1016/j.hydromet.2014.09.001.
[11] E. Ciro, A. Alzate, E. López, C. Serna, O. Gonzalez, Neodymium recovery from scrap magnet using ammonium persulfate, Hydrometallurgy 186 (2019) 226–234, https://doi.org/10.1016/j.hydromet.2019.04.016.
[12] C. Lupi, M. Pasquali, The electrolytic recovery of silver from photographic fixing baths the electrolytic recovery of silver from photographic fixing baths, in: D.B. Mishra, D.C. Ludwing, D.S. Das (Eds.), REWAS 2008, TMS (The Minerals, Metals & Materials Society), 2018, Cancun, Mexico, 2018, pp. 1427–1432.
[13] L. Rocchetti, A. Amato, F. Beolchini, Recovery of indium from liquid crystal displays, J. Clean. Prod. 116 (2016) 299–305, https://doi.org/10.1016/j.jclepro.2015.12.080.
[14] A. Amato, F. Beolchini, End of life liquid crystal displays recycling: a patent review, J. Environ. Manage. 225 (2018) 1–9, https://doi.org/10.1016/j.jenvman.2018.07.035.
[15] I.H. Kuong, J. Li, J. Zhang, X. Zeng, Estimating the evolution of urban mining resources in Hong Kong, up to the year 2050, Environ. Sci. Technol. 53 (2019) 1394–1403, https://doi.org/10.1021/acs.est.8b04063.
[16] Y. Li, Z. Liu, Q. Li, Z. Liu, L. Zeng, Recovery of indium from used indium – tin oxide (ITO) targets, Hydrometallurgy 105 (2011) 207–212, https://doi.org/10.1016/j.hydromet.2010.09.006.
[17] M.J. Jowkar, N. Bahaloo-horeh, S.M. Mousavi, Bioleaching of indium from discarded liquid crystal displays, J. Clean. Prod. 180 (2018) 417–429, https://doi.org/10.1016/j.jclepro.2018.01.136.
[18] S. Virolainen, D. Ibana, E. Paatero, Hydrometallurgy Recovery of indium from indium tin oxide by solvent extraction, Hydrometallurgy 107 (2011) 56–61, https://doi.org/10.1016/j.hydromet.2011.01.005.
[19] M. Souada, C. Louage, J. Doisy, L. Meunier, A. Benderrag, B. Ouddane, S. Bellayer, N. Nuns, M. Traisnel, U. Maschke, Ultrasonics - Sonochemistry Extraction of indium-tin oxide from end-of-life LCD panels using ultrasound assisted acid leaching, Ultrason. - Sonochemistry. 40 (2018) 929–936, https://doi.org/10.1016/j.ultsonch.2017.08.043.
[20] Y.F. Wu, Y.S. Wang, Indium recovery in an electrochemical flow reactor. Simulation and experiment, Int. J. Electrochem. Sci. 12 (2017) 3516–3536, https://doi.org/10.20964/2017.04.24.
[21] W. Chou, Y. Huang, Electrochemical removal of indium ions from aqueous solution using iron electrodes, J. Hazard. Mater. 172 (2009) 46–53, https://doi.org/10.1016/j.jhazmat.2009.06.119.
[22] M. Lee, Y. Oh, Analysis of ionic equilibria and electrowinning of indium from chloride solutions, Scand. J. Metall. 33 (2004) 279–285, https://doi.org/10.1111/j.1600-0692.2004.00693.x.
[23] E. Barrado, S. García, J.A. Rodríguez, Y. Castrillejo, Electrodeposition of indium on W and Cu electrodes in the deep eutectic solvent choline chloride-ethylene glycol (1:2), J. Electroanal. Chem. 823 (2018) 106–120, https://doi.org/10.1016/j.jelechem.2018.06.004.
[24] F.C. Walsh, D.R. Gabe, The electrodeposition of indium, Surf. Technol. 8 (1979) 87–99, https://doi.org/10.1016/0376-4583(79)90054-2.
[25] F.C. Walsh, D.R. Gabe, Electrode reactions during the electrodeposition of indium from acid sulphate solutions, Surf. Technol. 6 (1978) 425–436, https://doi.org/10.1016/0376-4583(78)90012-2.
[26] M.T. Hsieh, C.T. Chen, T.J. Whang, Triethanolamine-facilitated one-step electrodeposition of CuAlSe2 thin films and the mechanistic studies utilizing cyclic voltammetry, J. Electroanal. Chem. 762 (2016) 73–79, https://doi.org/10.1016/j.jelechem.2015.12.041.
[27] Q. Huang, K. Reuter, S. Amhed, L. Deligianni, L.T. Romankiw, Electrodeposition of indium on copper for CIS and CIGS solar cell applications, J. Electrochem. Soc. 158 (2011) D57–D61, https://doi.org/10.1149/1.3518440.
[28] D.Y. Gamburg, G. Zangari, Theory and Practice of Metal Electrodeposition, Springer, New York, NY, 2011, pp. 205–232.
[29] K.M. Yin, B.T. Lin, Effects of boric acid on the electrodeposition of iron, nickel and iron-nickel, Surf. Coatings Technol. 78 (1996) 205–210, https://doi.org/10.1016/0257-8972(94)02410-3.
[30] C. Ashworth, G. Frisch, Complexation equilibria of indium in aqueous chloride, sulfate and nitrate solutions: an electrochemical investigation, J. Solution Chem. 46 (2017) 1928–1940, https://doi.org/10.1007/s10953-017-0675-y.